Selection for Improved Energy Use Efficiency and Drought Tolerance in Canola Results in Distinct Transcriptome and Epigenome Changes[1][OPEN]

Aurine Verkest, Marina Byzova[2], Cindy Martens[2], Patrick Willems, Tom Verwulgen, Bram Slabbinck, Debbie Rombaut, Jan Van de Velde, Klaas Vandepoele, Evi Standaert, Marrit Peeters, Mieke Van Lijsebettens, Frank Van Breusegem*, and Marc De Block*

Department of Plant Systems Biology, VIB, 9052 Ghent, Belgium (A.V., M.B., C.M., P.W., T.V., B.S., D.R., J.V.d.V., K.V., M.V.L., F.V.B.); Department of Plant Biotechnology and Bioinformatics, Ghent University, 9052 Ghent, Belgium (A.V., M.B., C.M., P.W., T.V., B.S., D.R., J.V.d.V., K.V., M.V.L., F.V.B.); Bayer CropScience, 9052 Ghent, Belgium (C.M., E.S., M.P., M.D.B.); Department of Medical Protein Research, VIB, 9000 Ghent, Belgium (P.W.); and Department of Biochemistry, Ghent University, 9000 Ghent, Belgium (P.W.)

ORCID IDs: 0000-0003-3683-8537 (A.V.); 0000-0001-8445-9377 (M.B.); 0000-0003-4667-2294 (P.W.); 0000-0003-4790-2725 (K.V.); 0000-0002-7632-1463 (M.V.L.); 0000-0002-3147-0860 (F.V.B.); 0000-0003-0206-3825 (M.D.B.).

To increase both the yield potential and stability of crops, integrated breeding strategies are used that have mostly a direct genetic basis, but the utility of epigenetics to improve complex traits is unclear. A better understanding of the status of the epigenome and its contribution to agronomic performance would help in developing approaches to incorporate the epigenetic component of complex traits into breeding programs. Starting from isogenic canola (*Brassica napus*) lines, epilines were generated by selecting, repeatedly for three generations, for increased energy use efficiency and drought tolerance. These epilines had an enhanced energy use efficiency, drought tolerance, and nitrogen use efficiency. Transcriptome analysis of the epilines and a line selected for its energy use efficiency solely revealed common differentially expressed genes related to the onset of stress tolerance-regulating signaling events. Genes related to responses to salt, osmotic, abscisic acid, and drought treatments were specifically differentially expressed in the drought-tolerant epilines. The status of the epigenome, scored as differential trimethylation of lysine-4 of histone 3, further supported the phenotype by targeting drought-responsive genes and facilitating the transcription of the differentially expressed genes. From these results, we conclude that the canola epigenome can be shaped by selection to increase energy use efficiency and stress tolerance. Hence, these findings warrant the further development of strategies to incorporate epigenetics into breeding.

The need to improve crop yield in both quantity (yield potential) and stability (actual yield) to meet the increasing demand for food, feed, and plant-derived materials is a major challenge. Very different complementary technologies are used to optimize yield and to develop crops with increased resilience against adverse environmental growth conditions (Botella et al., 2008; Cattivelli et al., 2008; Jhaet al., 2014). Plant breeding programs are a basic component of this improvement process encompassing a wide range of technologies, such as exploration of the genetic potential by intraspecific and interspecific crosses, combination of genetic pools in hybrid breeding, mutational breeding, molecular breeding, and transgene technologies.

Rather recently, epigenetics has been investigated as a potential breeding platform (Springer, 2013). Epigenetic variations or heritable changes in gene expression that are not linked to changes in the DNA sequence, but associated with differences in DNA methylation or histone modifications, provide an alternative source of phenotypic variability. A vast and growing number of studies implicate DNA methylation and histone modification in the modulation of gene expression in general, control of developmental transitions, and plant responses to biotic

and abiotic stresses (He et al., 2003; Raissig et al., 2011; Dowen et al., 2012; Perrella et al., 2013). However, our current understanding of the stability and heritability of epigenetic variation is limited. As such, how to implement epigenetics-related strategies into breeding remains an open question.

In plants, transgenerational inheritance has been shown for single-gene epialleles, such as *SUPERMAN* (Jacobsen and Meyerowitz, 1997) and *CYCLOIDEA* (Cubas et al., 1999), and for a transcription factor (TF) that controls fruit ripening in tomato (*Solanum lycopersicum*; Manning et al., 2006). For complex traits, such as flowering time, plant height, and primary root length, stable transgenerational epigenetic variations could be induced and linked to the identification of epigenetic quantitative trait loci (Johannes et al., 2009; Cortijo et al., 2014). Additional evidence supporting the impact of transgenerational epigenetic variation in breeding and the concept of shaping the epigenome to improve complex traits has been provided (Hauben et al., 2009). Starting from an isogenic canola (*Brassica napus*) population, individual plants were selected for reduced respiration, and subsequently, the self-fertilized progeny with the highest energy use efficiency were retained. This step was repeated twice with the progeny obtained from the previous selection cycle to fix the epigenome and to select epigenetically altered progeny with distinct physiological and agronomical properties that remained stable for at least eight generations.

Here, selection for energy use efficiency (Hauben et al., 2009) and drought tolerance were combined to isolate epilines. To unravel the biology of the enhanced energy use efficiency and drought stress tolerance, alterations in the transcriptome and epigenome in two of these epilines as well as one of the energy use-efficient epilines, the previously described line LR77 (Hauben et al., 2009), were analyzed in depth at the physiological, biochemical, and molecular levels. The LR77 line will be referred to hereafter as the EUE line.

RESULTS

Selection of Canola Lines with Improved Drought Stress Tolerance

Epilines were generated from the doubled haploid Athena spring canola cultivar by a repeated selection procedure similar to that described previously (Hauben et al., 2009; De Block and Van Lijsebettens, 2011). By screening explants of isogenic lines, variations in complex traits in the isolated progeny are expected to result from epigenetic differences (epialleles). Hypocotyl explants from 2-week-old seedlings were evaluated for respiration, and the shoot tips were kept for rooting. To induce a moderate drought stress, the hypocotyl explants were cultured on medium containing 5% (w/v) polyethylene glycol (PEG) 6000. Under these conditions, the respiration of the hypocotyl explants was higher than that of explants grown without PEG. Rooted shoot tips from 10 seedlings with the lowest

hypocotyl explant respiration were transferred to the greenhouse for seed production by self-fertilization. Noteworthy, in this experimental setup, the plants were never exposed to PEG. Two of the self-fertilized progeny with the lowest respiration and the highest NAD(P)H content were retained. The selection procedure was repeated in three subsequent generations (Supplemental Fig. S1A). Respiration and NAD(P)H content were determined in the progeny of the last selection, and two epilines with low respiration and high NAD(P)H content, referred as the PEG1 and PEG2 lines, were kept for further analyses (Table I).

As described previously, lines with low respiration and high NAD(P)H content had reduced photorespiration (Hauben et al., 2009) under both control and PEG-induced stress conditions (Supplemental Table S1).

Under greenhouse conditions, the PEG lines could not be distinguished from the control plants regarding size, flowering time, and seed set. To assess their performance under drought stress, we subjected control and PEG plants to a drought stress regime starting on day 14 after sowing by withholding water supply until wilting symptoms (8 d) became apparent, followed by rewatering for 2 d. The PEG lines had increased rosette diameters (Fig. 1A). Under well-watered conditions, the shoot fresh weights were similar in PEG and control plants (Fig. 1B). The drought regime slowed down the growth of all lines, yet to a significantly smaller extent (25% versus 55% growth reduction) in the PEG lines, demonstrating an improved drought stress tolerance (Fig. 1B). The drought tolerance and energy use efficiency of the PEG lines were inherited stably for up to seven generations when seed upscaling was done by self-fertilization under nonselective conditions.

Nitrogen use efficiency (NUE) is an important agricultural trait that is possibly linked with drought tolerance (Sadras and Richards, 2014). The NUE of PEG and control lines was determined in a root length measurement assay on medium with low (35 μL L^{-1}) or standard (210 μL L^{-1}) nitrogen content. Plants with a high NUE form more lateral roots and have a higher total root length than plants with a low NUE. The seedlings of the PEG lines had a 40% higher total root length than control seedlings when grown on medium with low nitrogen content (Supplemental Fig. S1B).

Table I. *Respiration (TTC-H), energy content (NADH + NADPH), and energy use efficiency (EE) of hypocotyl explants*

Three repetitions per assay and 35 plants per repetition were used. Values shown are percentages versus control. EUE line data were as published by Hauben et al. (2009). Significance was determined by ANOVA with Dunnett's posttest: *, $P < 0.05$; **, $P < 0.01$; ***, and $P < 0.001$; TTC-H, reduced 2,3,5-triphenyltetrazolium chloride; ND, not determined.

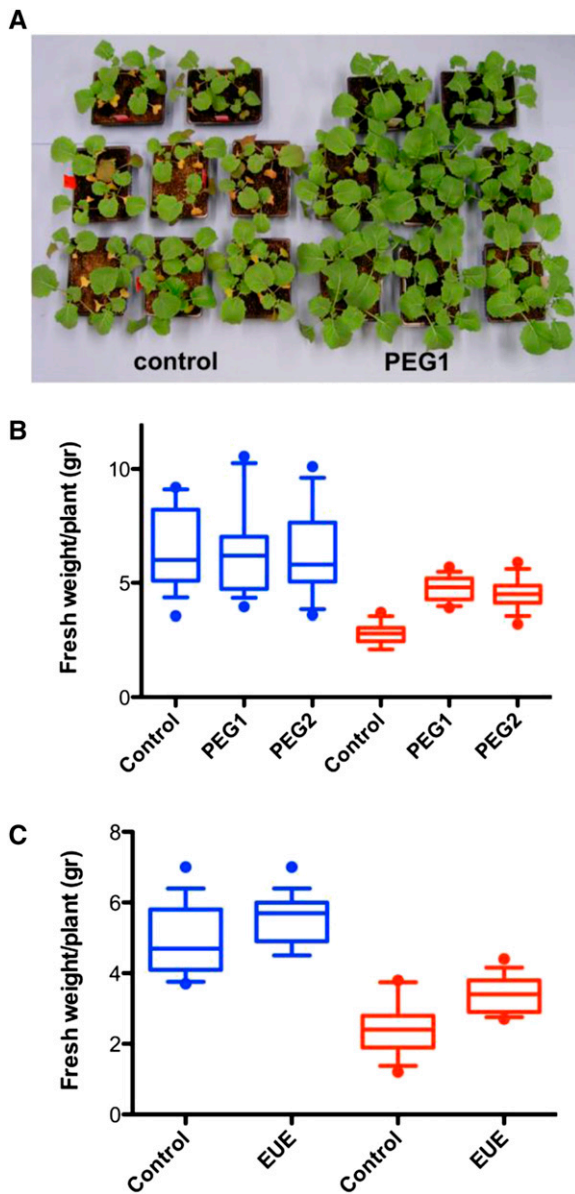| Lines	Control Conditions			+PEG		
	TTC-H	NAD(P)H	EE	TTC-H	NAD(P)H	EE
PEG1	91***	103*	113***	95***	114***	120***
PEG2	90***	99	110***	94***	108**	115***
EUE	92.5***	103*	111**	ND	ND	ND

Figure 1. Fresh weight of plants selected for high energy use efficiency (EUE lines) and drought tolerance (PEG lines). A, Control and PEG1 plants exposed to drought. The photograph was taken at the end of the experiment (24 d after sowing). For the experimental conditions, see "Materials and Methods." B and C, Box-plot comparisons of the fresh weight of control, PEG1, and PEG2 plants (B) and of control and EUE plants (C) grown under control (blue) and drought (red) conditions 24 d after sowing. The whiskers are at the 10th and 90th percentiles, and the horizontal bar in each box shows the mean.

In the EUE line, the seed yield was enhanced under optimal and moderate drought stress conditions, the photorespiration was reduced, the respiration had decreased, and the energy levels had increased. This line had been identified by selection for increased energy use efficiency and had been shown to have a decreased global DNA methylation level and altered histone modification patterns (Hauben et al., 2009). In this line,

the growth was reduced by only 40% compared with 55% in its control upon an identical drought treatment as used for the PEG lines, which was significant but less pronounced than that of the drought tolerance measured in the PEG lines (Fig. 1C). Whereas the PEG lines had a pronounced NUE, the EUE line did not form significantly more roots than the control on medium with low nitrogen content and, thus, did not use nitrogen more efficiently.

Gene Expression Changes in PEG and EUE Lines

To assess the molecular footprint caused by the selection procedures for increased energy use efficiency in the presence or absence of PEG and to identify candidate genes responsible for the enhanced drought tolerance phenotypes of the selected lines, we performed genome-wide transcriptome analyses on control and selected plants. Both PEG lines (two biological replicates) and EUE lines (three biological replicates) with their respective controls were analyzed. Actively transcribed polysomal RNA pools from plants in different biological replicate experiments were isolated and subjected to RNA sequencing (RNA-seq) analysis.

As a complete and annotated genome sequence for canola (AACC genome) is not available yet, the genomes of the diploid species *Brassica rapa* (turnip; AA) and *Brassica oleracea* (cabbage; CC), of which the hybridization formed the amphidiploid canola species, were used as reference sequences. To optimize the mapping efficiency, RNA-seq reads were mapped to a set of 60,756 nonredundant *B. rapa* and *B. oleracea* transcripts (see "Materials and Methods"). Details of the mapping efficiency and coding sequence coverage are provided in Supplemental Table S2. Genes with low read coverage (see "Materials and Methods") were excluded, finally retaining 35,892 genes (59% of all *B. rapa* and *B. oleracea* transcripts) to be examined. Differential transcript levels were identified using the edgeR package (false discovery rate < 0.05, fold change > 1.5; Robinson et al., 2010).

PEG1 plants displayed an altered expression in 1,158 genes, of which 706 induced and 452 repressed when compared with the control plants (Table II; Supplemental Table S3). In the PEG2 line, 478 genes were differentially expressed compared with the control line, of which 352 were up-regulated and 126 were down-regulated (Table II; Supplemental Table S3). The differential expression of arbitrarily selected genes was validated by quantitative reverse transcription-PCR (Fig. 2; Supplemental Table S4). The PEG1 and PEG2 lines displayed a significant overlap (355 genes; P < 1e-150) and a high expression correlation (r = 0.97) among the shared differentially expressed genes (DEGs; Fig. 2A), indicating that the selection altered the expression of a specific set of genes. In the EUE plants, screened solely for high energy use efficiency, a total of 1,099 DEGs were identified when compared with the corresponding control, among which 1,048 were up-regulated and 51 were down-regulated (Table II; Supplemental Table S2). Consistent with the

Table II. *RNA-seq results*

Line	Brassica spp. Lines[a]			Arabidopsis[b]		
	All	Up-Regulated	Down-Regulated	All	Up-Regulated	Down-Regulated
PEG1	1,158	706	452	844	503	341
PEG2	478	352	126	360	257	103
EUE	1,099	1,048	51	768	719	49

[a]Nonredundant *B. rapa* and *B. oleracea* genes.   [b]Unique orthologous genes.

partially similar selection strategy, a large number of DEGs (289 genes) were common in the EUE and PEG lines (Supplemental Fig. S2).

To gain insight into the functional categories of the DEGs, we used their Arabidopsis (*Arabidopsis thaliana*) orthologs as a proxy (Table II; Supplemental Table S3). For 83% of all *B. rapa* and *B. oleracea* genes, an Arabidopsis orthologous gene was found. Comparison of the classification of the Arabidopsis orthologs of PEG1, PEG2, and EUE of the DEGs in the Gene Ontology (GO) terms related to the biological processes and molecular functions revealed the overrepresentation of the same terms, as expected given the high number of shared genes (Fig. 2C; Supplemental Table S5). Signal transduction, response to stress, transport, TF activity, protein binding, and kinase activity terms were significantly (more than 1.5-fold; $P < 0.05$) enriched, suggesting the onset of signaling events related to stress tolerance adaptation (Fig. 2C; Supplemental Table S5).

Accordingly, the DEGs of the PEG and EUE lines (Arabidopsis proxies) used as input for the signature tool in Genevestigator (see "Materials and Methods"; Hruz et al., 2008) demonstrated the relatedness with stress-linked perturbation profiles (Supplemental Table S6), including several drought stress experiments. The highest relative drought similarity scores were observed with the PEG1 line, followed by PEG2 and EUE (Supplemental Table S6). These transcriptomic signatures were largely in agreement with the higher drought stress tolerance of the PEG lines than that of the EUE lines (Fig. 1, B and C) and confirm the efficient selection procedure in the presence of PEG. A subsequent hierarchical clustering of the RNA-seq data with the Arabidopsis water stress-related transcriptome data sets (Supplemental Table S7) allowed a more detailed comparative analysis (Fig. 2D; Supplemental Fig. S3). There is a clear correlation with salt, osmotic, abscisic acid (ABA), mannitol, and drought treatments provoking expression changes (Fig. 2D; Supplemental Fig. S3). Indeed, of the responsive PEG1, PEG2, and EUE genes, 67.3%, 64.3%, and 62.7% were differentially expressed, respectively, in at least two of the compared subselected data sets
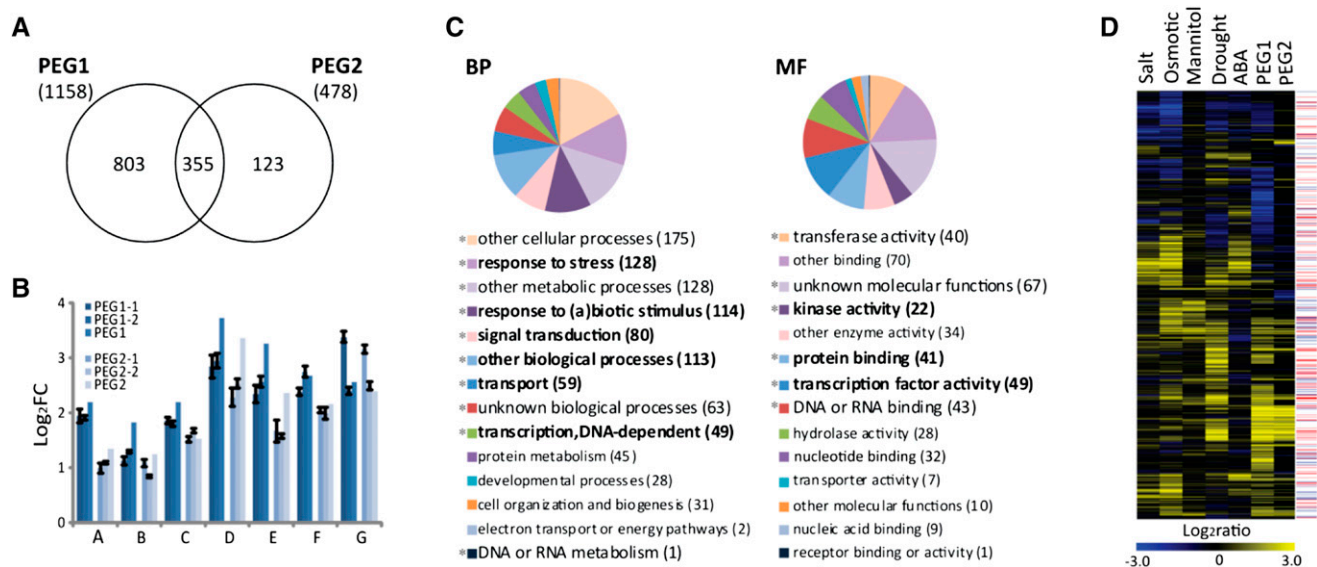
Figure 2. Transcriptome changes related to energy use efficiency and drought tolerance. A, Venn diagram of DEGs in the PEG1 and PEG2 lines. B, Quantitative reverse transcription-PCR validation of the DEGs. Values are means ± SD ($n = 3$). For PEG1 and PEG2, $\log_2$ fold change (FC) values were calculated from RNA-seq data. C, Functional categorization of shared DEGs by annotation for the GO biological process (BP) and molecular function (MF) categories. The enriched (greater than 1.5-fold) functional categories are in boldface. *, $P < 0.05$. D, Hierarchical clustering analysis of the PEG Arabidopsis orthologous genes and a subset of drought stress-related transcriptome data sets (24 h of salt/osmotic/mannitol/drought and 3 h of ABA; Supplemental Table S7). TF (red) or kinase (blue) functional GO annotations for individual genes are indicated on the right.

(24-h salt, 24-h osmotic, 24-h mannitol, 3-h ABA, and 24-h drought treatments), confirming that PEG and energy use efficiency selection target, at least in part, drought tolerance-linked pathways.

Altered Histone 3 Lysine-4 Trimethylation Distribution in the Drought-Tolerant Canola Line

To investigate the epigenetic effect on the histone mark distribution of the energy use efficiency/PEG selection, we performed a chromatin immunoprecipitation sequencing (ChIP-seq) analysis. Dynamic changes in the occurrence of the histone 3 lysine-4 trimethylation (H3K4me3) mark are associated with the regulation of drought stress-responsive gene expression (Kim et al., 2008; Ding et al., 2012; Sani et al., 2013). Native ChIP with an anti-H3K4me3 antibody and without antibody (background control) was done on PEG1 and control plants. Details of the sequencing and mapping to the *B. rapa* and *B. oleracea* genomes separately are provided in Supplemental Table S8. The H3K4me3 distribution and differential binding in control and PEG1 lines were analyzed with the model-based analysis of chromatin immunoprecipitation sequencing (MACS; Zhang et al., 2008).

Using the MACS callpeak module, H3K4me3-enriched *B. rapa* and *B. oleracea* regions were identified in both the control and PEG1 lines and annotated to the nearest neighboring gene (Table III; Supplemental Tables S9 and S10). As expected for a histone protein modification, a uniform distribution of H3K4me3 was observed across all chromosomes of *B. rapa* (Fig. 3) and *B. oleracea* (Supplemental Fig. S4). More detailed analysis of the genomic H3K4me3 distribution in both *B. oleracea* and *B. rapa* in relation to the linked genes revealed that 26.2% of the enriched regions were located at the 5′ side (1 kb or intergenic), 66.2% in gene bodies, and 7.6% in the 3′ overlapping region (Supplemental Tables S9 and S10). A total of 73.4% of the H3K4me3 marks were located in the 5′ 1-kb (19.3%) and 5′ coding (54.1%) regions (Fig. 3B), consistent with the H3K4me3 distribution reported in Arabidopsis (Zhang et al., 2009; Roudier et al., 2011).

For differential H3K4me3 distribution analysis, the MACS bdgdiff module was used (see "Materials and Methods"). Comparison of the MACS callpeak-generated H3K4me3 pileup tracks of the control and PEG1 lines revealed that the majority of the H3K4me3-bound regions were common and not significantly different between the two lines (Fig. 3A; Supplemental Fig. S4). A few regions displayed an enhanced H3K4me3 signal in the control line, but many appeared enriched in

H3K4me3 signal in the PEG1 line (Table III; Fig. 3A; Supplemental Fig. S4; Supplemental Tables S11 and S12). The above analyses were done on one biological replicate, because the H3K4me3 association of different regions was validated by quantitative PCR after ChIP on independent biological replicates of plant material of the control, PEG1, and PEG2 lines. For all regions, enrichment was higher in the PEG1 line than in the control, confirming the differential H3K4me3 binding and illustrating that PEG selection alters the H3K4me3 distribution (Fig. 3C). Moreover, enriched binding was seen in the PEG2 line in the same regions as those found in the PEG1 line (Fig. 3C), suggesting that the episelection directs the H3K4me3 alteration of a specific set of genes. Remarkably, six out of the eight genes with an enriched binding in the PEG1 line were also enriched in the PEG2 line. That not all the tested genes give an enriched binding in the PEG2 line can be explained by the weaker drought tolerance of the PEG2 line than that of the PEG1 line (Fig. 1B), as also reflected in the RNA-seq analyses (see above).

Annotation of the PEG1-enriched H3K4me3 regions to the nearest gene, followed by functional enrichment analysis of the Arabidopsis orthologous genes, uncovered overrepresented GO terms similar to the DEGs (Fig. 3D; Supplemental Tables S5, S11, and S12), further demonstrating the selectivity of the energy use efficiency and PEG selection toward stress tolerance-related signaling processes. In agreement, exploration of the Arabidopsis drought stress-related transcriptomes (Supplemental Table S7) revealed substantial changes in the PEG1 H3K4me3-enriched or differentially H3K4me3-marked (DHM) orthologs (Supplemental Fig. S5). Approximately 45% of the DHMs were differentially expressed in the osmotic treatment (24-h) data set, representing a significantly higher percentage of all osmotic treatment-responsive genes than that of the PEG1 DEGs (20% versus 6%) and indicating that the DHM distribution targets additional drought stress-responsive genes (Supplemental Fig. S5). Together, our data demonstrate that the PEG lines display DHM distribution and that this epigenetic factor may constitute a causative factor of the increased PEG drought stress performance.

Interdependence of Differential Gene Expression and H3K4me3 Distribution

As the presence of specific histone marks might directly affect gene expression, the DHM data were searched for genes that were differentially expressed in the PEG1 line. In total, both data sets shared 219 genes

Table III. *Number of total and differentially H3K4me3-bound regions (and genes) identified in PEG1 and control plants*

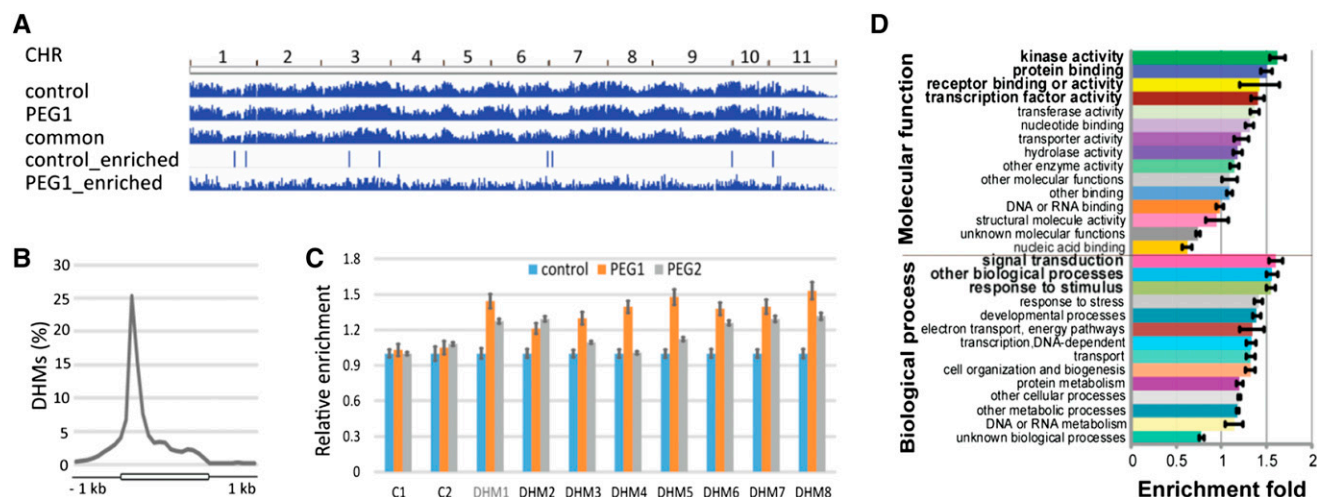| Species	Total Regions (Genes)		Differential Regions (Genes)	
	Control	PEG1	Control Enriched	PEG1 Enriched
B. rapa	27,673 (21,844)	31,464 (23,925)	8 (8)	3,131 (2,872)
B. oleracea	36,371 (26,617)	40,707 (28,492)	38 (36)	1,806 (1,748)

Figure 3. Genome-wide H3K4me3 distribution in the PEG lines. A, H3K4me3 distribution across the 11 *B. rapa* chromosomes (CHR). B, Gene body and flanking 1-kb region distribution of the H3K4me3 marks in *B. oleracea* and *B. rapa*. All genes were aligned from start to end and divided into 20 equal bins. Upstream and downstream 1-kb regions were divided into 10 equal bins. C, ChIP-quantitative PCR validation of enriched H3K4me3 binding (DHM genes) in PEG1 and PEG2 lines. The relative enrichment compared with the control was determined using two ChIP-seq-identified nonenriched regions (C1 and C2). Error bars indicate SD ($n = 3$). D, Functional categorization of PEG1-enriched H3K4me3 genes by annotation for the GO biological process and molecular function categories. The enriched (greater than 1.5-fold) functional categories are in boldface ($P < 0.05$).

(Fig. 4; Supplemental Table S13), revealing a small but significant overlap ($P = 4.9e-10$). Comparative analysis of this overlapping subset of genes with the Arabidopsis abiotic stress transcriptome data sets (Supplemental Table S7) strengthened, as confirmed by the GO classification, the link with the drought stress response and the overrepresentation of TFs and kinases (Fig. 4B; Supplemental Table S5). Among the differentially expressed TFs, the *B. oleracea* (ERC) *ERC42165*, *B. rapa* (ERF) *ERF62736*, and *ERF5709* loci, encoding the *Brassica WRKY33, ETHYLENE-RESPONSIVE FACTOR104 (ERF104)*, and *NO APICAL MERISTEM, ARABIDOPSIS TRANSCRIPTION ACTIVATION FACTOR, AND CUP-SHAPED COTYLEDON090* orthologs, respectively, were found to be enriched with H3K4me3. Read coverage along the 5′ coding regions in the PEG1 sample was higher than that of the control (Fig. 4D). Likewise, enriched H3K4me3 occupancy was detected in the 5′ regions of *ERC26284* and *ERF77038* loci, the *Brassica* spp. *MITOGEN-ACTIVATED PROTEIN KINASE KINASE9* and *CREATINE PHOSPHOKINASE32* orthologs (Fig. 4D). In agreement with the described connection of H3K4me3 with gene activation (Roudier et al., 2011), most (76.7%) of the differentially marked genes were up-regulated (Fig. 4, B and C; Supplemental Table S13). Surprisingly, part of the H3K4me3-enriched genes appeared to be down-regulated in both the PEG1 line and the Arabidopsis drought stress-related expression profiling data (Fig. 4B). Interestingly, repressed genes, in contrast to induced ones, displayed an atypical H3K4me3 enrichment at the 3′ ends of transcripts (Supplemental Fig. S6). This unanticipated distribution and its effect on the expression of the generally considered activating H3K4me3 mark needs further investigation.

Previously, a role for H3K4me3 in gene repression was reported (Weiner et al., 2012). Altogether, these data suggest that the differential H3K4me3 distribution sensitizes the PEG lines to enhanced drought stress tolerance, partly by directly affecting the expression of stress tolerance genes.

Identifying Drought-Related Signaling Networks

The enrichment of both kinases and TFs in the RNA-seq (DEG) and ChIP-seq (DHM) data sets and in their overlap (DHM+DEG; Figs. 2, C and D, 3D, and 4B; Supplemental Fig. S5; Supplemental Table S5) hints at a regulatory role in conferring the improved drought stress tolerance phenotypes. In the DEG and DHM+DEG data sets, there is a significant enrichment in kinases that are involved in osmotic stress signaling events, such as class I receptor-like, class IV calcium response (group 4.2), and mitogen-activated protein (groups 4.1 and 4.5) kinases (http://plantsp.genomics.purdue.edu; Supplemental Table S14; Marshall et al., 2012; Kissoudis et al., 2014). The TF classification shows an overrepresentation of primarily the APETALA2-ETHYLENE-RESPONSIVE ELEMENT-BINDING PROTEIN (AP2-EREBP) and WRKY families (Supplemental Table S15; Lindemose et al., 2013). Screening of the 1,000-bp upstream promoter regions of all DEGs and DHM genes for the W-box, DROUGHT-RESPONSIVE (DRE) elements, and ABSCISIC ACID-RESPONSIVE (ABRE) motifs identified putative WRKY, AP2-EREBP DEHYDRATION-RESPONSIVE ELEMENT BINDING (DREB) family, and basic Leu zipper TFs downstream of drought-responsive

Figure 4. Relationship between the differential H3K4me3 distribution and the transcript levels. A, Venn diagram of the annotated DHM genes and DEGs in the PEG1 line. B, Clustering of orthologous DEGs and DHM genes of Arabidopsis with drought stress-related transcriptome data sets (24 h of salt/osmotic/mannitol/drought and 3 h of ABA; Supplemental Table S7). TF (red) and kinase (blue) functions of GO annotations for individual genes are indicated on the right. C, Box-plot displaying the log$_2$ fold change (FC) expression of the H3K4me3-enriched genes of the PEG1 line. D, Genome-View representation (Abeel et al., 2012) of selected DEGs and DHM genes showing the read coverage in PEG1 versus the control line. The reads are piled up with forward reads above and reverse reads below the axis. Total coverage is gray shaded. Scaling was done relative to the maximum number of reads. The read number is given in the middle of the enriched regions. The coding regions are indicated as gray boxes and the PEG1-enriched regions as pink boxes above the reads. Bars = 0.5 kb.
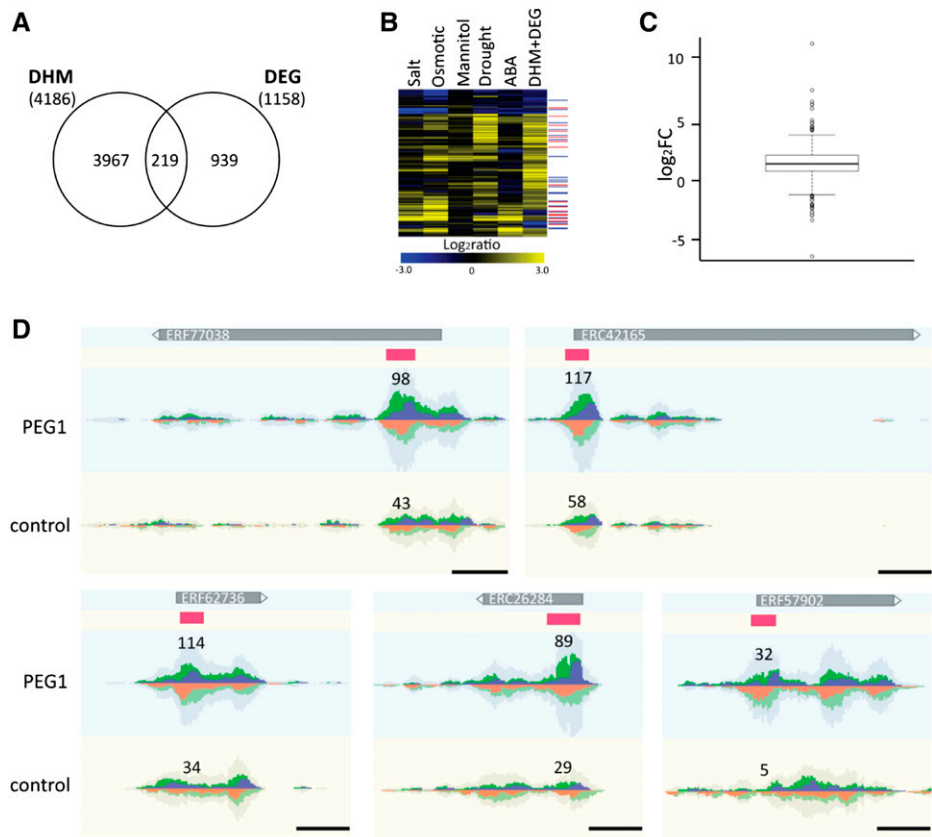
genes (see "Materials and Methods"). The number and identity of the DEGs and DHM genes retrieved by both simple and conserved noncoding sequence (CNS)-based mapping (Van de Velde et al., 2014) of these cis-regulatory elements are provided in Supplemental Table S16. Regarding the DEGs, 55.1%, including 23.7% high-confidence CNS-displaying DEGs, appeared to be putative target genes, whereas for the DHM+DEG genes, higher mapping fractions were observed, namely 61.6% simple and 18.9% CNS-based targets. Moreover, DEGs and DHM genes containing W-box, DRE sites, and ABRE motifs retained TF, kinase, and drought stress-associated GO term enrichments. In addition, a significant overrepresentation for all three motifs was evident in the CNS-based DEG and DHM genes (Fig. 5; Supplemental Table S16), confirming roles for WRKY, AP2-EREBP DREB, and basic Leu zipper TFs as master regulators in the energy use efficiency/PEG selection-improved drought stress tolerance signaling.

To gain a hierarchical insight into the signaling and regulatory events, we used the DEG and DHM genes as query genes to retrieve pairwise regulatory (motif) interactions, protein interactions, and kinase-substrate interactions from the literature and several databases (see "Materials and Methods"; De Bodt et al., 2012; Zulawski et al., 2013; Jones et al., 2014; Lumba et al., 2014; Van de Velde et al., 2014). From the resulting 3,987 pairwise interactions, an integrative network was constructed,

linking 1,841 genes/proteins (44.6% of all DEGs and DHMs). The generated network included 289 TFs that regulate 1,143 downstream DEGs and DHM genes and 190 kinases that interact with 125 proteins and phosphorylate 203 targets (Supplemental Table S17). Clustering (see "Materials and Methods") allowed the isolation and closer inspection of discrete subnetworks. The most extensive subnetwork, comprising 875 genes/proteins, illustrated the high connectivity between the DEGs and DHM genes and retained GO term enrichments for TF and kinase activity (Supplemental Fig. S7). Interestingly, we observed a significant overrepresentation of genes displaying responses to water deprivation, to osmotic and salt stresses, and to ABA stimulus (Supplemental Fig. S7). When first-neighbor interactions of individual genes were extracted, PEG1 differentially expressed and/or H3K4me3-enriched kinases and TFs also appear as main regulators in several drought stress tolerance-related subnetworks (Fig. 5B; Supplemental Fig. S8; Supplemental Table S17). As an example, the network of WRKY53, a mitogen-activated protein kinase substrate, displays, besides regulatory interactions with other WRKY TFs, links with the dehydration stress-responsive TFs ERF5 and MYB15 and the REGULATORY COMPONENTS OF ABSCISIC ACID RECEPTOR1 (Miao et al., 2004; Ding et al., 2009; Park et al., 2009; Dubois et al., 2013; Fig. 5B). Moreover, WRKY53 is known to be regulated by histone methylation (Ay et al., 2009).
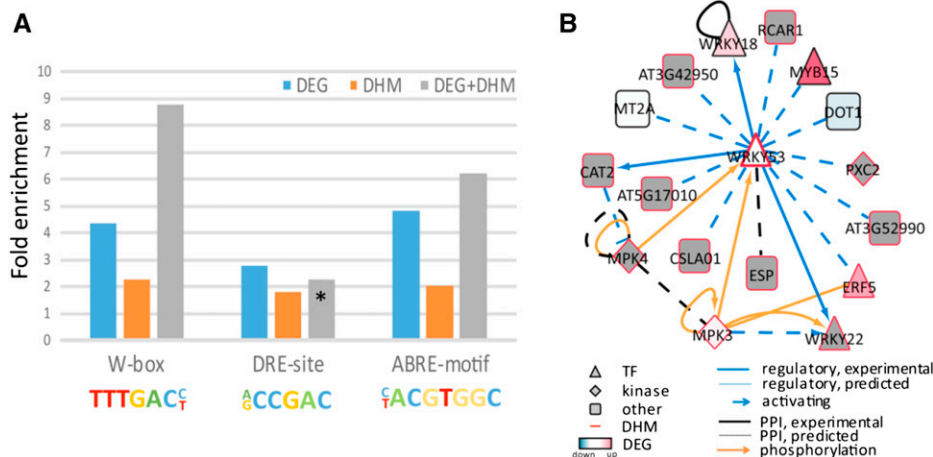
Figure 5. Network analysis of DEGs enriched in H3K4me3. A, Cis-regulatory element enrichment analysis using 1-kb promoter sequences. Enrichment of W-box, DRE site, and ABRE motif occurrence in conserved noncoding sequences upstream of DEGs and/or DHM genes. Sequence logos used in mapping are shown below the graph. *, Not significant ($P > 0.05$). B, Gene regulatory and interaction subnetwork. The module represents pairwise first-neighbor interactions of the WRKY53 TFs with other PEG1 DEGs and/or DHM genes (see "Materials and Methods"; Supplemental Table S17). PPI, Protein-protein interaction.

Together, these analyses support a model (Fig. 6) in which DEG and DHM key genes, primarily TFs and kinases, regulate downstream responses. Considering the role of the H3K4me3 dynamics in drought stress gene responsiveness (Kim et al., 2008; Ding et al., 2012), the strong regulatory interconnection observed among DEGs and DHM genes (Supplemental Fig. S7) suggests that the cascade conferring the improved drought stress tolerance in the PEG epilines becomes activated upon stress exposure (Fig. 6; Supplemental Fig. S8).

DISCUSSION

Epigenetic Selection for Energy Use Efficiency and Drought Tolerance

Molecular analysis of selected energy use-efficient (EUE) lines and drought-tolerant (PEG lines) plants highlights the directed epigenome and transcriptome changes and provides evidence for the episelection and an explanation for the enhanced drought stress tolerance of the epilines. RNA-seq analysis of control and PEG lines demonstrated the modified expression of a specific set of genes. In two independently selected PEG lines, a high overlap of shared DEGs was observed. Moreover, functional annotation and comparison with Arabidopsis transcriptome studies revealed a significant representation of genes linked to osmotic stress and ABA signaling. In favor of the efficiency of the combined selection strategy for both energy use efficiency and drought tolerance, the differential gene expression profiles of the PEG lines correlated better with water deprivation stress data than the EUE line selected solely for high energy use efficiency. Interestingly, the altered gene expression rendered the PEG lines more drought stress tolerant without negatively affecting growth or yield under optimal conditions (as observed in field trials), making them promising candidates for engineering enhanced stress tolerance.

The repeated selection for energy use efficiency solely or energy use efficiency and drought tolerance over several generations starting from isogenic populations of canola is an effective and fast process: from a population of approximately 200 plants, stable epilines with the selected phenotype were obtained after three generations. The altered gene expression in both the EUE and PEG lines obtained by screening explants of isogenic plants that are maintained and taken to the next generation when displaying the desired trait suggests an epigenetic feature. As already shown (Hauben et al., 2009), this screening resulted in the isolation of genetically identical, but epigenetically different, canola populations that were transgenerationally stable for over eight generations with respect to their phenotypes. Here, we demonstrate that this selection strategy enables the modulation of stress genes in the absence of a stimulus, indicating that the transgenerational trait inheritance occurs independently of any priming and memory (Molinier et al., 2006; Whittle et al., 2009). Similar to the EUE line, the drought tolerance of the PEG lines was inherited stably
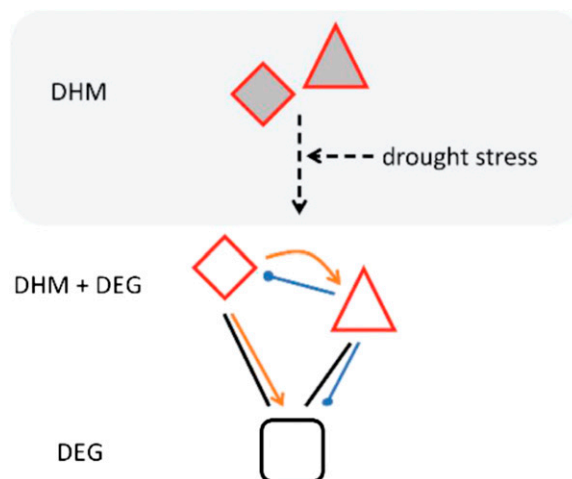

Figure 6. Proposed network by CORNET (see "Materials and Methods") conferring drought stress tolerance in the PEG epilines. Nodes depict DEGs (white) and/or DHM genes (red border), with triangles and diamonds representing TFs and kinases, respectively.

over at least seven generations. In isogenic populations, the epigenome is diverse and undergoes dynamic changes. During the screening process, some of these epigenetic states, epialleles, could be selected and fixed. Fixation of epialleles will reduce the epigenetic variation of the selected phenotype/trait in the population, as can be seen by the narrowing of the variation of the selected phenotype/trait in the population after each selection cycle (Hauben et al., 2009). It is very unlikely that mutations are responsible for the selected phenotypes, because the line to which the selections were applied was a double haploid that was derived from a single microspore and was maintained under controlled conditions to avoid unwanted cross-pollinations. After each seed upscaling, the progeny were tested for purity using specific phenotypic and molecular markers. Moreover, the high frequencies with which the epilines were selected (10^{-2}) make selection by mutation very improbable. To assess potential genomic differences between a selected epiline and the original control line from which the epiline was derived, a variant-calling procedure was done on the available RNA-seq data of the PEG1 line and its control. Very few DNA polymorphisms were identified that probably do not cause mutations underlying the selected phenotypes (Supplemental Text S1).

Transcript Levels and H3K4me3 in the Epilines

The effectiveness of the episelection strategy was supported by the ChIP-seq analysis of control and PEG1 plants. Functional annotation of the H3K4me3-enriched genes in PEG1 plants and comparison with Arabidopsis transcriptome studies confirmed a significant representation of osmotic stress-linked genes. Moreover, in the PEG2 line, several regions with enriched H3K4me3 binding corresponded with those found in the PEG1 line, further favoring the specificity of the PEG selection to fix certain epialleles. In plants, changes in histone methylation mark distribution have been implicated in response to a range of abiotic stresses, including drought, osmotic, and salt stresses (Sokol et al., 2007; van Dijk et al., 2010; Kim et al., 2012; Sani et al., 2013; Zong et al., 2013). In all these studies, histone mark changes resulted from sensitization for stress responsiveness. In contrast, our selection strategy isolated epilines with a directed altered H3K4me3 distribution under optimal nonprimed conditions: only the hypocotyl explants of the seedlings were used for screening stress tolerance, whereas the shoot tips that were rooted and transferred to the greenhouse were never exposed to the stress. More research is needed to understand the mechanism of the epiallele selection, fixation, and transgenerational inheritance, for example by studying the epigenome of the populations generated in the three subsequent selections steps.

In plants, a positive correlation has been found between H3K4me3 and gene transcription (Roudier et al., 2011). Accordingly, most DEGs with enriched H3K4me3 mark distribution are up-regulated in the PEG lines.

However, until now, it has been unclear whether the H3K4me3 pattern is the cause or the consequence of the increased gene expression (Sani et al., 2013). Besides the overall positive correlation between H3K4me3 and gene expression, a small set of down-regulated PEG genes also display H3K4me3 enrichment. The lack of correlation between H3K4me3 and enhanced gene expression was also described in other studies (Weiner et al., 2012; Sani et al., 2013). Moreover, the positive correlation between H3K4me3 and gene expression is much weaker for genes with a high expression than for those with a low expression (Sani et al., 2013). In budding yeast (*Saccharomyces cerevisiae*), a repressive role for H3K4me3 has been reported (Weiner et al., 2012). A limited, but substantial, set of diamide stress-repressed genes were found to have increased H3K4me3 levels. Interestingly, this unexpected chromatin mark enrichment appeared to target a specific gene class, the ribosomal protein genes (Weiner et al., 2012). Among the small number of H3K4me3-enriched transcriptionally repressed PEG genes (47 genes), no specific gene group seems overrepresented. Notably, whereas H3K4me3 occurs at the 5′ ends of transcribed and PEG-induced genes, the repressed PEG genes displayed an atypical H3K4me3 enrichment distribution at the 3′ ends. This unanticipated distribution and its possible effect on expression need further investigation. Additionally, studies might connect the H3K4me3 enrichment of PEG lines with osmotic stress-responsive up-regulated and, possibly, down-regulated genes.

Chromatin modification is not necessarily correlated directly with transcriptional regulation, but it can generate a context for the interplay with other factors at a developmental stage or in an environmental condition. Elevated H3K4me3 levels may not affect transcription immediately, but could act as preparatory/sensitizing marks for a fast and genome-wide gene transcription responsiveness upon stress perception (Jaskiewicz et al., 2011). Considering the high number of H3K4me3-enriched osmotic stress-responsive genes without altered expression in the PEG1 line, examination and comparison of their expression profiles upon stress exposure might be interesting. In summary, our study demonstrates that epilines with distinct characteristics can be selected from a pool of isogenic seeds, implying that the implementation of epigenetics in breeding is promising.

MATERIALS AND METHODS

Plant Material, Generation of Lines, and Physiological and Biochemical Analyses

Athena is an elite canola (*Brassica napus*) breeding line of Bayer CropScience. Canola lines with improved energy use efficiency and drought stress tolerance were selected as described previously with some minor modifications (Hauben et al., 2009). Seedlings from an isogenic doubled haploid line were grown for 2 weeks on agar in one-half-strength Murashige and Skoog medium supplemented with 2% (w/v) Suc. Seedling shoot tips were placed on the medium for rooting, whereas five hypocotyl explants per seedling were cultured for 5 d on callus-inducing medium containing 5% (w/v) PEG-6000 (Fluka BioUltra; Sigma-Aldrich) before cellular

respiration was measured (Hauben et al., 2009). Rooted shoot tips of seedlings with the lowest respiration were transferred to the greenhouse for seed production by self-fertilization and subjected to two additional identical selection rounds. Respiration and photorespiration of the obtained lines were measured as described (Hauben et al., 2009).

Intracellular NADH and NADPH were quantified as described (Nakamura et al., 2003) with the following modifications. For the reaction solution, 5% (v/v) of the Cell Counting Kit-8 (Dojindo Laboratories) was diluted in 25 mM potassium phosphate buffer (pH 7.4) containing 0.1 mM 1-methoxyphenazine methosulfate (Sigma-Aldrich) and 0.1% (v/v) PEG sorbitan monolaurate (Tween 20). The explants were placed in the reaction solution and incubated at 26°C for 30 min to 1 h. The absorbance of the reaction solution was measured at 450 nm [optical density at 450 nm = 0.281 for 10 μM NAD(P)H].

NUE was scored by quantifying the root formation on medium with a low nitrogen content (35 μL L^{-1}) versus medium with a standard nitrogen content (210 μL L^{-1}). Hoagland medium (Hoagland and Arnon, 1938) with 1.2% (w/v) plant agar (Duchefa) was poured into square Nunc bioassay dishes (Thermo Scientific). After solidification of the agar, the top half of the medium was removed and seeds were sown on top of the agar layer. The plates were incubated vertically for 8 d (at 23°C, 80 μmol m^{-2} s^{-1} light, and a 16-h-light/8-h-dark regime). The roots that grew on the surface of the agar were quantified by scanning the plates and analyzed with ImageJ (http://imagej.nih.gov/ij/).

Drought tolerance was analyzed by measuring the fresh weight of shoots of 24-d-old normally watered and drought regime-treated plants. After 13 d, plants under the drought regime were no longer watered for 8 d, until wilting symptoms became apparent, followed by watering for 2 d, after which the fresh weight was determined.

Polysomal RNA Isolation

Polysomal RNA was isolated according to an adapted protocol (de Jong et al., 2006). Ground and liquid nitrogen frozen material of leaf 4 from 26-d-old control and selected lines was solubilized in an equal volume of extraction buffer (pH 8.5) containing 0.2 M Tris, 0.1 M KCl, 70 mM magnesium acetate, 50 mM EGTA, 0.25 M Suc, 10 mM dithiothreitol, 100 μg mL^{-1} cycloheximide (Sigma-Aldrich), and 100 units mL^{-1} SUPERase-In (Ambion). The slurry was allowed to thaw on ice and gently mixed to enhance homogenization. The suspension was strained through two layers of Miracloth (Merck Millipore) via successive centrifugation for 1 min at 100g (4°C) and 5 min at 1,000g (4°C) in 50-mL sterile tubes. The cleared supernatant was centrifuged for 15 min at 8,400g (4°C) to pellet additional debris, made to 1% (v/v) Triton X-100, and incubated on ice for 10 min. After centrifugation at 20,800g (4°C) in an Eppendorf tabletop centrifuge, the supernatant was loaded in SW41 Ultra-Clear tubes (Beckman Coulter) on discontinuous Suc gradients that consisted of 0.6 mL of 1.65 M Suc and 1 mL of 1 M Suc, both buffered with 10× concentrated Suc salt buffer (pH 8.5, autoclaved) containing 0.4 M Tris, 1 M KCl, 0.3 M magnesium acetate, and 50 mM EGTA. To maintain RNA integrity, 10 mM dithiothreitol, 100 μg mL^{-1} cycloheximide, and 100 units mL^{-1} SUPERase-In (Ambion) were added to these Suc solutions. The gradients were centrifuged for 4 h at 150,000g (4°C) in an ultracentrifuge (type L8-50 M/E; Beckman Coulter) to pellet the polysomes. The polysomal pellets were resuspended in 100 μL of extraction buffer, and polysomal RNA was isolated with an RNeasy kit (Qiagen). The quantity of polysomal RNA was measured with a Nanodrop spectrophotometer (Thermo Scientific), and the quality was examined with a Bioanalyzer 2100 (Agilent Technologies) and the RNA 6000 Nano Assay kit (Agilent Technologies).

RNA-seq Analysis

The RNA-seq analysis was done at the Beijing Genome Institute. Complementary DNA (cDNA) sequencing libraries were prepared from polysomal RNA by means of the mRNA-Seq Sample Preparation Kit (Illumina) and run on a genome analyzer (GAIIx; Illumina), yielding 90-bp paired-end reads that were quality controlled with FastQC (version 0.10.0; http://www.bioinformatics.bbsrc.ac.uk/projects/fastqc/), which showed that the quality decreased in the last 10 bp of the reads. With the FASTX trimmer of the FASTX toolkit (version 0.0.13; http://hannonlab.cshl.edu/fastx_toolkit/), 10 bases were trimmed at the 3' side, yielding high-quality 80-bp paired-end reads.

As a reference for the read mapping, a nonredundant gene set was built as follows. Orthologous pairs were formed by an all-against-all BLASTN (Altschul et al., 1990) comparison between the nucleotide sequences of the in silico predicted gene sequences of *Brassica rapa* and *Brassica oleracea* (in-house data) and by retrieval of the reciprocal best hits, resulting in 21,260 orthologous

pairs and 39,496 singletons (nonorthologs). Because of the higher annotation quality of *B. rapa*, the *B. rapa* ortholog was taken as the orthologous pair representative in every orthologous pair. These 21,260 orthologous pair representatives together with the 39,496 singletons form the nonredundant reference gene set that contains 60,756 genes.

In the next step, the high-quality 80-bp paired-end reads were mapped to the nonredundant gene set with GSNAP [unique mapping with maximum number of paths to print set to 1 (-n 1 -Q) and maximum of five mismatches (-m 5) allowed]. These options enforce, when used together, that reads that cannot be mapped in a unique manner, are not written to the output file (Wu and Nacu, 2010). All reads were retained that mapped uniquely and concordantly, and the number of reads mapping to each transcript was calculated with samtools idxstats (Li et al., 2009). The corresponding count table was filtered on a minimum average read count of five over the lines analyzed and then was given as an input to edgeR (Robinson et al., 2010) for differential expression testing.

Quantitative Reverse Transcription-PCR

Total RNA was extracted with the RNeasy Plant Mini Kit (Qiagen) and treated with DNase I prior to cDNA synthesis. cDNA was prepared from DNase I-treated total RNA with the iScript cDNA Synthesis Kit (Bio-Rad) according to the manufacturer's instructions. The relative transcript abundance of selected genes (for genes and primers used, see Supplemental Table S4) was determined with the LightCycler 480 system and the LC480 SYBR Green I Master kit (Roche Diagnostics). Two biological and three technical repeats were measured. To obtain relative expression values, the amplification data were analyzed by means of qBase+ (Hellemans et al., 2007) with the second derivative maximum method and three reference genes for normalization.

Native ChIP

The native ChIP protocol was adapted (Bernatavichute et al., 2008) as follows. Material from leaf 4 of 26-d-old wild-type and PEG1 plants was harvested, frozen in liquid nitrogen, and ground to powder (1.5 g). Plant tissue was resuspended in 15 mL of HBM buffer (25 mM Tris-HCl, pH 7.5, 440 mM Suc, 10 mM MgCl$_2$, 0.1% [v/v] Triton-X, 10 mM β-mercaptoethanol, 2 mM spermine, 1 mM phenylmethanesulfonyl fluoride [PMSF], 1 μg mL^{-1} pepstatin, 1 μg mL^{-1} aprotinin, and 1 μg mL^{-1} leupeptin), homogenized, and filtered twice through Miracloth (Merck Millipore). After centrifugation at 1,000g for 5 min (4°C; SS-34 Sorvall; Thermo Scientific), the pellet was resuspended in 5 mL of NIB buffer (20 mM Tris-HCl, pH 7.5, 250 mM Suc, 5 mM MgCl$_2$, 5 mM KCl, 0.1% [v/v] Triton-X, 10 mM β-mercaptoethanol, 1 mM PMSF, 1 μg mL^{-1} pepstatin, 1 μg mL^{-1} aprotinin, and 1 μg mL^{-1} leupeptin), applied to a 15%/50% Percoll (GE-Healthcare) gradient in NIB buffer, and centrifuged at 500g for 20 min (4°C; SS-34 Sorvall). Isolated nuclei were washed three times in NIB buffer and flash frozen in liquid nitrogen in HBC buffer (25 mM Tris-HCl, pH 7.5, 440 mM Suc, 10 mM MgCl$_2$, 0.1% [v/v] Triton-X, 10 mM β-mercaptoethanol, and 20% [v/v] glycerol). Nuclei from each preparation were diluted 2-fold in digestion buffer (20 mM Tris-HCl, pH 7.5, 0.22 M Suc, 50 mM NaCl, 5 mM MgCl$_2$, 1 mM CaCl$_2$, and 5 mM sodium butyrate), centrifuged at 600g for 5 min (4°C; model 5415R; Eppendorf), and resuspended in 0.25 mL of digestion buffer for micrococcal nuclease (30 units; Affymetrix) digestion for 10 min at 37°C stopped with 10 mM EDTA. Mononucleosomes were released by treating nuclei with 0.1% (v/v) Triton-X for 2 h in the cold and then pelleting the debris by centrifugation at 9,300g for 5 min (4°C; 5415R; Eppendorf). The supernatants were diluted to 0.5 mL in incubation buffer (20 mM Tris-HCl, pH 7.5, 50 mM NaCl, 5 mM EDTA, 0.1% [v/v] Triton-X, 20 mM sodium butyrate, 0.1 mM PMSF, 1 μg mL^{-1} pepstatin, 1 μg mL^{-1} aprotinin, and 1 μg mL^{-1} leupeptin) and incubated overnight in the cold with and without 2.5 μg of the anti-H3K4m3 antibody (#07-473; Merck Millipore). Then, 50 μL of Dynabeads Protein G (Invitrogen) was added, incubated for 3 h in the cold, and washed three times with 500 μL of wash buffer (50 mM Tris-HCl, pH 7.5, 10 mM EDTA, 5 mM sodium butyrate, 0.1 mM PMSF, 1 μg mL^{-1} pepstatin, 1 μg mL^{-1} aprotinin, and 1 μg mL^{-1} leupeptin) with increasing concentrations of NaCl (50, 100, and 150 mM) subsequently. The final wash was done in TE buffer (10 mM Tris-Cl, pH 8, 500 mM NaCl, and 1 mM EDTA), and immunocomplexes were eluted and reverse cross-linked by incubation overnight at 65°C in 0.25 mL of 10 mM Tris-HCl (pH 8), 1 mM EDTA, 0.5 M NaCl, 1% (w/v) SDS, and 1 μL of RNase A (100 mg mL^{-1}). Eluates were incubated with 100 μg of Proteinase K for 2 h at 42°C, and the DNA was extracted by phenol/chloroform/indole-3-acetic acid, followed by

purification with the Qiaquick PCR purification kit and DNA quantification with the Quant-iT dsDNA High Sensitivity kit (Invitrogen).

ChIP-seq Analysis

ChIP DNA libraries were prepared according to the manufacturer's protocol and sequenced on a HiSeq2500 (100 paired-end reads; Illumina). The sequencing data were quality controlled with FastQC. Overrepresented sequences were removed using FASTX-clipper from the FASTX toolkit. The reads were mapped to the reference genomes of *B. rapa* and *B. oleracea* using GSNAP with default settings (Wu and Nacu, 2010). Reads that could not be assigned to a unique position in the genome were removed.

Peak calling was done with MACS version 2.0 (Zhang et al., 2008). The genome size (-g) was set at 2.0e8 and 3.7e8 for *B. rapa* and *B. oleracea*, respectively. Other parameters were set at their default values using the BAMPE format option. For differential histone mark-binding analysis, the MACS version 2.0 bdgdiff module with default settings was used. Peaks were annotated by overlapping the peak summits reported by MACS with the *B. rapa* or *B. oleracea* annotation. A peak was assigned to the closest gene, taking into account both upstream and downstream regions of the genes. When a peak was located within the boundaries of a gene, it was assigned to this gene.

Quantitative ChIP-PCR

Quantitative PCR experiments were carried out on H3K4me3 ChIP-isolated genomic DNA from control and selected epilines and done as technical triplicates on equal DNA concentrations with the LightCycler 480 system and the LC480 SYBR Green I Master kit (Roche Diagnostics). Primers used for PCR amplification were designed surrounding the mid region of nonenriched (C1 and C2) and enriched regions identified by the sequencing (Supplemental Table S4). ChIP values of H3K4me3 binding were normalized by means of nonenriched regions.

Computational Analyses

The overlap significance of gene sets was calculated with a hypergeometric distribution test. Orthologous Arabidopsis genes (The Arabidopsis Information Resource 10) of the *B. rapa* and *B. oleracea* genes were identified by an all-against-all BLASTN (E-value cutoff of 1e-5; Altschul et al., 1990) and by retrieval of the reciprocal best hits. Functional GO classification and enrichment analysis of the Arabidopsis orthologs were done with BAR (Toufighi et al., 2005) and PLAZA 2.5 (Van Bel et al., 2012).

For comparative transcriptome analysis, the Genevestigator signature tool was utilized and hierarchical clustering analyses were performed. The 300 strongest DEGs (highest absolute $\log_2$ fold changes) were extracted separately for the PEG1, PEG2, and EUE lines and used as input for the signature tool in Genevestigator (Hruz et al., 2008), thereby selecting all perturbation experiments on the ATH1 microarray platform (relative $\log_2$ fold scaled data) to retrieve similar experiments. Raw Affymetrix Cell Intensity files were obtained from the Gene Expression Omnibus database (ncbi.nlm.nih.gov/geo/; GSE5628, GSE5621, GSE5622, GSE5623, GSE39384, GSE16474, GSE36789, and GSE22107) and ArrayExpress (ebi.ac.uk/arrayexpress/; E-MEXP-2435 and E-MEXP-2377). Data were normalized with Robust Multiarray Average (Bolstad et al., 2003; Irizarry et al., 2003a, 2003b) with the affy package of R/Bioconductor (Gautier et al., 2004). Probe sets were annotated according to the latest Brainarray (http://brainarray.mbni.med.umich.edu/Brainarray/; Dai et al., 2005) custom chip definition file provided for Arabidopsis (The Arabidopsis Information Resource G version 18.0.0). Differential gene expression was analyzed by the limma package (Smyth, 2004). Genes were hierarchically clustered (single linkage) by Pearson correlation in the open-source analysis software MultiExperiment Viewer version 4.9.0 (Saeed et al., 2003).

Genes were annotated as TFs when found at least twice in the databases DATF (Guo et al., 2005), PlnTFDB (Pérez-Rodríguez et al., 2010), AtTFDB (Yilmaz et al., 2011), and PlantTFDB (Jin et al., 2014). For the annotation of kinases, the PlantsP database (Tchieu et al., 2003) was used.

For promoter analysis, sequences were restricted to the first 1,000 bp upstream from the translation start site or to a shorter region when the adjacent upstream gene was located at a distance smaller than 1,000 bp. Known motifs from the integrated AGRIS, PLACE, and AthaMap (Van de Velde et al., 2014) databases were mapped with the dna-pattern program without allowing mismatches (Thomas-Chollier et al., 2008).

For network analysis, Arabidopsis orthologous DHM genes and DEGs were used as query genes to retrieve pairwise interaction information from different sources. Protein-protein interactions were extracted from CORNET2.0 (De Bodt et al., 2012; cornet.psb.ugent.be/) using experimental and predicted interactions from all available databases. Predicted interactions were filtered to a minimum of two independent references. Additional protein interaction sources were MIND (Jones et al., 2014; associomics.org/), eTRAIN (Lumba et al., 2014), and kinase-substrate interactions from PhosPhAt4.0 (Zulawski et al., 2013; phosphat.uni-hohenheim.de/). Regulatory interactions were downloaded from AGRIS (Yilmaz et al., 2011; Arabidopsis.med.ohio-state.edu/) and supplemented with predicted conserved TF motif interactions (Van de Velde et al., 2014). Interactions were filtered on a minimum of two independent references (confirmed; AGRIS) and motif conservation among four species. Additional regulatory interactions were retrieved from the EVEX database (Van Landeghem et al., 2012; evexdb.org/). All interactions were loaded into Cytoscape, and the FAG-EC algorithm (Li et al., 2008) was run with default settings for network clustering.

The data discussed in this article have been deposited in the National Center for Biotechnology Information Gene Expression Omnibus (Edgar et al., 2002) and are accessible through the Gene Expression Omnibus accession number GSE65578.

Supplemental Data

The following supplemental materials are available.

Supplemental Figure S1. PEG line selection scheme and NUE analysis.

Supplemental Figure S2. Comparative transcriptome analysis of EUE and PEG plants.

Supplemental Figure S3. Hierarchical clustering analysis of RNA-seq and Arabidopsis drought stress-related transcriptome studies.

Supplemental Figure S4. H3K4me3 distribution across the *B. oleracea* reference.

Supplemental Figure S5. Heat map of differential expression levels of the Arabidopsis orthologous DHM genes in drought stress-related transcriptome data sets and the PEG1 line.

Supplemental Figure S6. Enriched H3K4me3 mark distribution in DEGs of PEG1.

Supplemental Figure S7. Cytoscape representation of the largest module obtained by clustering of the compiled interactome, kinase substrate, and regulatory data of the PEG1 DEGs and/or enriched DHM genes.

Supplemental Figure S8. Gene regulatory and interaction subnetwork of the CREATINE PHOSPHOKINASE32 kinase.

Supplemental Table S1. Photorespiration of selected epilines.

Supplemental Table S2. RNA-seq mapping details.

Supplemental Table S3. DEGs in the PEG and EUE lines.

Supplemental Table S4. List of primers.

Supplemental Table S5. Functional categorization of DEGs and DHM genes.

Supplemental Table S6. Genevestigator similarity analysis report of the DEGs of the PEG and EUE lines.

Supplemental Table S7. Arabidopsis transcriptome data sets (used for generating Supplemental Table S6).

Supplemental Table S8. ChIP-seq count and mapping results.

Supplemental Table S9. H3K4me3 distribution in the PEG control line.

Supplemental Table S10. H3K4me3 distribution in the PEG1 line.

Supplemental Table S11. H3K4me3 enrichment in the PEG control line.

Supplemental Table S12. H3K4me3 enrichment in the PEG1 line.

Supplemental Table S13. List of DEGs and DHM genes in the PEG1 line.

Supplemental Table S14. Kinase classification and enrichments.

Supplemental Table S15. Transcription factor classification and enrichments.

Supplemental Table S16. Simple and conserved cis-regulatory motif mapping.

Supplemental Table S17. List of pairwise protein and regulatory interactions between DEGs and/or DHM genes.

Supplemental Text S1. Variant calling between the PEG1 line and its control.

LITERATURE CITED

Abeel T, Van Parys T, Saeys Y, Galagan J, Van de Peer Y (2012) GenomeView: a next-generation genome browser. Nucleic Acids Res **40**: e12

Altschul SF, Gish W, Miller W, Myers EW, Lipman DJ (1990) Basic local alignment search tool. J Mol Biol **215**: 403–410

Ay N, Irmler K, Fischer A, Uhlemann R, Reuter G, Humbeck K (2009) Epigenetic programming via histone methylation at *WRKY53* controls leaf senescence in *Arabidopsis thaliana*. Plant J **58**: 333–346

Bernatavichute YV, Zhang X, Cokus S, Pellegrini M, Jacobsen SE (2008) Genome-wide association of histone H3 lysine nine methylation with CHG DNA methylation in *Arabidopsis thaliana*. PLoS ONE **3**: e3156

Bolstad BM, Irizarry RA, Åstrand M, Speed TP (2003) A comparison of normalization methods for high density oligonucleotide array data based on variance and bias. Bioinformatics **19**: 185–193

Botella MA, Rosada A, Bressan RA, Hasegawa PM (2008) Plant adaptive responses to salinity stress. *In* MA Jenks, PM Hasegawa, eds, Plant Abiotic Stress. Blackwell, Oxford, pp 37–70

Cattivelli L, Rizza F, Badeck FW, Mazzucotelli E, Mastrangelo AM, Francia E, Marè C, Tondelli A, Stanca AM (2008) Drought tolerance improvement in crop plants: an integrated view from breeding to genomics. Field Crops Res **105**: 1–14

Cortijo S, Wardenaar R, Colomé-Tatché M, Gilly A, Etcheverry M, Labadie K, Caillieux E, Hospital F, Aury JM, Wincker P, et al (2014) Mapping the epigenetic basis of complex traits. Science **343**: 1145–1148

Cubas P, Vincent C, Coen E (1999) An epigenetic mutation responsible for natural variation in floral symmetry. Nature **401**: 157–161

Dai M, Wang P, Boyd AD, Kostov G, Athey B, Jones EG, Bunney WE, Myers RM, Speed TP, Akil H, et al (2005) Evolving gene/transcript definitions significantly alter the interpretation of GeneChip data. Nucleic Acids Res **33**: e175

De Block M, Van Lijsebettens M (2011) Energy efficiency and energy homeostasis as genetic and epigenetic components of plant performance and crop productivity. Curr Opin Plant Biol **14**: 275–282

De Bodt S, Hollunder J, Nelissen H, Meulemeester N, Inzé D (2012) CORNET 2.0: integrating plant coexpression, protein–protein interactions, regulatory interactions, gene associations and functional annotations. New Phytol **195**: 707–720

de Jong M, van Breukelen B, Wittink FR, Menke FLH, Weisbeek PJ, Van den Ackerveken G (2006) Membrane-associated transcripts in Arabidopsis: their isolation and characterization by DNA microarray analysis and bioinformatics. Plant J **46**: 708–721

Ding Y, Fromm M, Avramova Z (2012) Multiple exposures to drought 'train' transcriptional responses in *Arabidopsis*. Nat Commun **3**: 740

Ding Z, Li S, An X, Liu X, Qin H, Wang D (2009) Transgenic expression of *MYB15* confers enhanced sensitivity to abscisic acid and improved drought tolerance in *Arabidopsis thaliana*. J Genet Genomics **36**: 17–29

Dowen RH, Pelizzola M, Schmitz RJ, Lister R, Dowen JM, Nery JR, Dixon JE, Ecker JR (2012) Widespread dynamic DNA methylation in response to biotic stress. Proc Natl Acad Sci USA **109**: E2183–E2191

Dubois M, Skirycz A, Claeys H, Maleux K, Dhondt S, De Bodt S, Vanden Bossche R, De Milde L, Yoshizumi T, Matsui M, et al (2013) ETHYLENE RESPONSE FACTOR6 acts as a central regulator of leaf growth under water-limiting conditions in Arabidopsis. Plant Physiol **162**: 319–332

Edgar R, Domrachev M, Lash AE (2002) Gene Expression Omnibus: NCBI gene expression and hybridization array data repository. Nucleic Acids Res **30**: 207–210

Gautier L, Cope L, Bolstad BM, Irizarry RA (2004) affy: analysis of *Affymetrix GeneChip* data at the probe level. Bioinformatics **20**: 307–315

Guo A, He K, Liu D, Bai S, Gu X, Wei L, Luo J (2005) DATF: a database of *Arabidopsis* transcription factors. Bioinformatics **21**: 2568–2569

Hauben M, Haesendonckx B, Standaert E, Van Der Kelen K, Azmi A, Akpo H, Van Breusegem F, Guisez Y, Bots M, Lambert B, et al (2009) Energy use efficiency is characterized by an epigenetic component that can be directed through artificial selection to increase yield. Proc Natl Acad Sci USA **106**: 20109–20114

He Y, Michaels SD, Amasino RM (2003) Regulation of flowering time by histone acetylation in *Arabidopsis*. Science **302**: 1751–1754

Hellemans J, Mortier G, De Paepe A, Speleman F, Vandesompele J (2007) qBase relative quantification framework and software for management and automated analysis of real-time quantitative PCR data. Genome Biol **8**: R19

Hoagland DR, Arnon DI (1938) The water-culture method for growing plants without soil. Calif Agric Exp Stn Circ **347**: 1–39

Hruz T, Laule O, Szabo G, Wessendorp F, Bleuler S, Oertle L, Widmayer P, Gruissem W, Zimmermann P (2008) Genevestigator v3: a reference expression database for the meta-analysis of transcriptomes. Adv Bioinformatics **2008**: 420747

Irizarry RA, Bolstad BM, Collin F, Cope LM, Hobbs B, Speed TP (2003a) Summaries of Affymetrix GeneChip probe level data. Nucleic Acids Res **31**: e15

Irizarry RA, Hobbs B, Collin F, Beazer-Barclay YD, Antonellis KJ, Scherf U, Speed TP (2003b) Exploration, normalization, and summaries of high density oligonucleotide array probe level data. Biostatistics **4**: 249–264

Jacobsen SE, Meyerowitz EM (1997) Hypermethylated *SUPERMAN* epigenetic alleles in *Arabidopsis*. Science **277**: 1100–1103

Jaskiewicz M, Conrath U, Peterhänsel C (2011) Chromatin modification acts as a memory for systemic acquired resistance in the plant stress response. EMBO Rep **12**: 50–55

Jha UC, Bohra A, Singh NP (2014) Heat stress in crop plants: its nature, impacts and integrated breeding strategies to improve heat tolerance. Plant Breed **133**: 679–701

Jin J, Zhang H, Kong L, Gao G, Luo J (2014) PlantTFDB 3.0: a portal for the functional and evolutionary study of plant transcription factors. Nucleic Acids Res **42**: D1182–D1187

Johannes F, Porcher E, Teixeira FK, Saliba-Colombani V, Simon M, Agier N, Bulski A, Albuisson J, Heredia F, Audigier P, et al (2009) Assessing the impact of transgenerational epigenetic variation on complex traits. PLoS Genet **5**: e1000530

Jones AM, Xuan Y, Xu M, Wang RS, Ho CH, Lalonde S, You CH, Sardi MI, Parsa SA, Smith-Valle E, et al (2014) Border control: a membrane-linked interactome of *Arabidopsis*. Science **344**: 711–716

Kim JM, To TK, Ishida J, Matsui A, Kimura H, Seki M (2012) Transition of chromatin status during the process of recovery from drought stress in *Arabidopsis thaliana*. Plant Cell Physiol **53**: 847–856

Kim JM, To TK, Ishida J, Morosawa T, Kawashima M, Matsui A, Toyoda T, Kimura H, Shinozaki K, Seki M (2008) Alterations of lysine modifications on the histone H3 N-tail under drought stress conditions in *Arabidopsis thaliana*. Plant Cell Physiol **49**: 1580–1588

Kissoudis C, van de Wiel C, Visser RGF, van der Linden G (2014) Enhancing crop resilience to combined abiotic and biotic stress through the dissection of physiological and molecular crosstalk. Front Plant Sci **5**: 207

Li H, Handsaker B, Wysoker A, Fennell T, Ruan J, Homer N, Marth G, Abecasis G, Durbin R (2009) The Sequence Alignment/Map format and SAMtools. Bioinformatics **25**: 2078–2079

Li M, Wang J, Chen J (2008) A fast agglomerate algorithm for mining functional modules in protein interaction networks. *In* YF Peng, YF Zhang, eds, BioMedical Engineering and Informatics: New Development and the Future, Vol 1. Institute of Electrical and Electronics Engineers, Los Alamitos, CA, pp 3–7

Lindemose S, O'Shea C, Jensen MK, Skriver K (2013) Structure, function and networks of transcription factors involved in abiotic stress responses. Int J Mol Sci **14**: 5842–5878

Lumba S, Toh S, Handfield LF, Swan M, Liu R, Youn JY, Cutler SR, Subramaniam R, Provart N, Moses A, et al (2014) A mesoscale abscisic acid hormone interactome reveals a dynamic signaling landscape in *Arabidopsis*. Dev Cell **29**: 360–372

Manning K, Tör M, Poole M, Hong Y, Thompson AJ, King GJ, Giovannoni JJ, Seymour GB (2006) A naturally occurring epigenetic

mutation in a gene encoding an SBP-box transcription factor inhibits tomato fruit ripening. Nat Genet **38:** 948–952

Marshall A, Aalen RB, Audenaert D, Beeckman T, Broadley MR, Butenko MA, Caño-Delgado AI, de Vries S, Dresselhaus T, Felix G, et al (2012) Tackling drought stress: RECEPTOR-LIKE KINASES present new approaches. Plant Cell **24:** 2262–2278

Miao Y, Laun T, Zimmermann P, Zentgraf U (2004) Targets of the WRKY53 transcription factor and its role during leaf senescence in *Arabidopsis*. Plant Mol Biol **55:** 853–867

Molinier J, Ries G, Zipfel C, Hohn B (2006) Transgeneration memory of stress in plants. Nature **442:** 1046–1049

Nakamura J, Asakura S, Hester SD, de Murcia G, Caldecott KW, Swenberg JA (2003) Quantitation of intracellular NAD(P)H can monitor an imbalance of DNA single strand break repair in base excision repair deficient cells in real time. Nucleic Acids Res **31:** e104

Park SY, Fung P, Nishimura N, Jensen DR, Fujii H, Zhao Y, Lumba S, Santiago J, Rodrigues A, Chow TF, et al (2009) Abscisic acid inhibits type 2C protein phosphatases via the PYR/PYL family of START proteins. Science **324:** 1068–1071

Pérez-Rodríguez P, Riaño-Pachón DM, Corrêa LG, Rensing SA, Kersten B, Mueller-Roeber B (2010) PlnTFDB: updated content and new features of the plant transcription factor database. Nucleic Acids Res **38:** D822–D827

Perrella G, Lopez-Vernaza MA, Carr C, Sani E, Gosselé V, Verduyn C, Kellermeier F, Hannah MA, Amtmann A (2013) Histone Deacetylase Complex1 expression level titrates plant growth and abscisic acid sensitivity in *Arabidopsis*. Plant Cell **25:** 3491–3505

Raissig MT, Baroux C, Grossniklaus U (2011) Regulation and flexibility of genomic imprinting during seed development. Plant Cell **23:** 16–26

Robinson MD, McCarthy DJ, Smyth GK (2010) edgeR: a Bioconductor package for differential expression analysis of digital gene expression data. Bioinformatics **26:** 139–140

Roudier F, Ahmed I, Bérard C, Sarazin A, Mary-Huard T, Cortijo S, Bouyer D, Caillieux E, Duvernois-Berthet E, Al-Shikhley L, et al (2011) Integrative epigenomic mapping defines four main chromatin states in Arabidopsis. EMBO J **30:** 1928–1938

Sadras VO, Richards RA (2014) Improvement of crop yield in dry environments: benchmarks, levels of organisation and the role of nitrogen. J Exp Bot **65:** 1981–1995

Saeed AI, Sharov V, White J, Li J, Liang W, Bhagabati N, Braisted J, Klapa M, Currier T, Thiagarajan M, et al (2003) TM4: a free, open-source system for microarray data management and analysis. Biotechniques **34:** 374–378

Sani E, Herzyk P, Perrella G, Colot V, Amtmann A (2013) Hyperosmotic priming of *Arabidopsis* seedlings establishes a long-term somatic memory accompanied by specific changes of the epigenome. Genome Biol **14:** R59

Smyth GK (2004) Linear models and empirical Bayes methods for assessing differential expression in microarray experiments. Stat Appl Genet Mol Biol **3:** Article 3

Sokol A, Kwiatkowska A, Jerzmanowski A, Prymakowska-Bosak M (2007) Up-regulation of stress-inducible genes in tobacco and *Arabidopsis*

cells in response to abiotic stresses and ABA treatment correlates with dynamic changes in histone H3 and H4 modifications. Planta **227:** 245–254

Springer NM (2013) Epigenetics and crop improvement. Trends Genet **29:** 241–247

Tchieu JH, Fana F, Fink JL, Harper J, Nair TM, Niedner RH, Smith DW, Steube K, Tam TM, Veretnik S, et al (2003) The PlantsP and PlantsT functional genomics databases. Nucleic Acids Res **31:** 342–344

Thomas-Chollier M, Sand O, Turatsinze JV, Janky R, Defrance M, Vervisch E, Brohée S, van Helden J (2008) RSAT: regulatory sequence analysis tools. Nucleic Acids Res **36:** W119–W127

Toufighi K, Brady SM, Austin R, Ly E, Provart NJ (2005) The Botany Array Resource: e-Northerns, Expression Angling, and promoter analyses. Plant J **43:** 153–163

Van Bel M, Proost S, Wischnitzki E, Movahedi S, Scheerlinck C, Van de Peer Y, Vandepoele K (2012) Dissecting plant genomes with the PLAZA comparative genomics platform. Plant Physiol **158:** 590–600

Van de Velde J, Heyndrickx KS, Vandepoele K (2014) Inference of transcriptional networks in *Arabidopsis* through conserved noncoding sequence analysis. Plant Cell **26:** 2729–2745

van Dijk K, Ding Y, Malkaram S, Riethoven JJM, Liu R, Yang J, Laczko P, Chen H, Xia Y, Ladunga I, et al (2010) Dynamic changes in genome-wide histone H3 lysine 4 methylation patterns in response to dehydration stress in *Arabidopsis thaliana*. BMC Plant Biol **10:** 238

Van Landeghem S, Hakala K, Rönnqvist S, Salakoski T, Van de Peer Y, Ginter F (2012) Exploring biomolecular literature with EVEX: connecting genes through events, homology, and indirect associations. Adv Bioinformatics **2012:** 582765

Weiner A, Chen HV, Liu CL, Rahat A, Klien A, Soares L, Gudipati M, Pfeffner J, Regev A, Buratowski S, et al (2012) Systematic dissection of roles for chromatin regulators in a yeast stress response. PLoS Biol **10:** e1001369

Whittle CA, Otto SP, Johnston MO, Krochko JE (2009) Adaptive epigenetic memory of ancestral temperature regime in *Arabidopsis thaliana*. Botany **87:** 650–657

Wu TD, Nacu S (2010) Fast and SNP-tolerant detection of complex variants and splicing in short reads. Bioinformatics **26:** 873–881

Yilmaz A, Mejia-Guerra MK, Kurz K, Liang X, Welch L, Grotewold E (2011) AGRIS: the Arabidopsis Gene Regulatory Information Server, an update. Nucleic Acids Res **39:** D1118–D1122

Zhang X, Bernatavichute YV, Cokus S, Pellegrini M, Jacobsen SE (2009) Genome-wide analysis of mono-, di- and trimethylation of histone H3 lysine 4 in *Arabidopsis thaliana*. Genome Biol **10:** R62

Zhang Y, Liu T, Meyer CA, Eeckhoute J, Johnson DS, Bernstein BE, Nusbaum C, Myers RM, Brown M, Li W, et al (2008) Model-based analysis of ChIP-Seq (MACS). Genome Biol **9:** R137

Zong W, Zhong X, You J, Xiong L (2013) Genome-wide profiling of histone H3K4-tri-methylation and gene expression in rice under drought stress. Plant Mol Biol **81:** 175–188

Zulawski M, Braginets R, Schulze WX (2013) PhosPhAt goes kinases: searchable protein kinase target information in the plant phosphorylation site database PhosPhAt. Nucleic Acids Res **41:** D1176–D1184